

Supplementary information

Proteomic signaling of dual specificity phosphatase 4 (DUSP4) in Alzheimer's disease

Table of Contents

Supplementary methods	2
Supplementary results and discussion	4
Supplementary figures legends	5
Supplementary data list	22
References	22

Supplementary methods

Proteomics/phosphoproteomics sample preparation

Each tissue sample was added to 300 μ L of urea lysis buffer (8 M urea, 10 mM Tris, 100 mM NaH_2PO_4 , pH 8.5, including 3 μ L (100x stock) HALT(-EDTA) protease and phosphatase inhibitor cocktail (Pierce)) in a 1.5 mL Rino tube (Next Advance) harboring stainless steel beads (0.9-2 mm in diameter). Samples were homogenized twice for 5-minute intervals in the cold room (4 °C). Protein homogenates were transferred to 1.5 mL Eppendorf tubes on ice and were sonicated (Sonic Dismembrator, Fisher Scientific) 3 times for 5 sec each with 5 sec intervals of rest at 30% amplitude to disrupt nucleic acids and were subsequently centrifuged at 4° C. Protein concentration was determined by the bicinchoninic acid (BCA) method, and samples were frozen in aliquots at -80 °C. Protein homogenates (500 μ g) were treated with 5 mM dithiothreitol (DTT) at room temperature for 30 min, followed by 10 mM iodoacetamide at room temperature for 30 min in the dark. Protein samples were digested with 1:25 (w/w) lysyl endopeptidase (Wako) at room temperature overnight. Next day, samples were diluted with 50 mM NH_4HCO_3 to a final concentration of less than 2 M urea and were further digested overnight with 1:25 (w/w) trypsin (Promega) at room temperature. The resulting peptides were desalted with HLB column (Waters) and were dried under vacuum.

Phosphopeptide enrichment

Ten µg peptide was reserved for total proteome measurement and rest of the peptide was subjected to phosphopeptide enrichment using Thermo Scientific High-Select™ Fe-NTA Phosphopeptide Enrichment Kit. Dried peptides were submitted for mass spectrometry.

LC-MS/MS analysis

The data acquisition by LC-MS/MS was adapted from a published procedure¹. Derived peptides were resuspended in the loading buffer (0.1% trifluoroacetic acid, TFA) and were separated on a Waters Charged Surface Hybrid (CSH) column (150 µm internal diameter (ID) x 15 cm; particle size: 1.7 µm). The samples were run on an EVOSEP liquid chromatography system using the 15 samples per day preset gradient (88 min) and were monitored on a Q-Exactive Plus Hybrid Quadrupole-Orbitrap Mass Spectrometer (ThermoFisher Scientific). The mass spectrometer cycle was programmed to collect one full MS scan followed by 20 data dependent MS/MS scans. The MS scans (400-1600 m/z range, 3×10^6 AGC target, 100 ms maximum ion time) were collected at a resolution of 70,000 at m/z 200 in profile mode. The HCD MS/MS spectra (1.6 m/z isolation width, 28% collision energy, 1×10^5 AGC target, 100 ms maximum ion time) were acquired at a resolution of 17,500 at m/z 200. Dynamic exclusion was set to exclude previously sequenced precursor ions for 30 seconds. Precursor ions with +1, and +7, +8 or higher charge states were excluded from sequencing.

MaxQuant analysis

Label-free quantification analysis was adapted from a published procedure¹. Spectra were searched using the search engine Andromeda, integrated into MaxQuant, against 2020 Uniprot/Swiss-Prot mouse database (17,041 target sequences). Serine, threonine, and tyrosine phosphorylation (+79.9663 Da), methionine oxidation (+15.9949 Da), asparagine and glutamine deamidation (+0.9840 Da), and protein N-terminal acetylation (+42.0106 Da) were variable modifications (up

to 5 allowed per peptide); cysteine was assigned as a fixed carbamidomethyl modification (+57.0215 Da). Only fully tryptic peptides were considered with up to 2 missed cleavages in the database search. A precursor mass tolerance of ± 20 ppm was applied prior to mass accuracy calibration and ± 4.5 ppm after internal MaxQuant calibration. Other search settings included a maximum peptide mass of 6,000 Da, a minimum peptide length of 6 residues, 0.05 Da tolerance for orbitrap and 0.6 Da tolerance for ion trap MS/MS scans. The false discovery rate (FDR) for peptide spectral matches, proteins, and site decoy fraction were all set to 1 percent. Quantification settings were as follows: re-quantify with a second peak finding attempt after protein identification has completed; match MS1 peaks between runs; a 0.7 min retention time match window was used after an alignment function was found with a 20-minute RT search space. Quantitation of proteins was performed using summed peptide intensities given by MaxQuant. The quantitation method only considered razor plus unique peptides for protein level quantitation.

DESeq2 analysis

The RNA-seq raw read quality control and preprocessing are as described in ². Differentially expressed genes were identified using the R package DESeq2³. The input count matrix was the read counts summarized at the gene level per sample. Pre-filtering was used to screen out low count genes so that only genes with at least 2 reads, in total, across the samples in each comparison were kept. Differential expression analysis was performed using the DESeq function, followed by the log fold change shrinkage⁴ via the type of apegglm. To be consistent with DEP identification, we defined differentially expressed genes (DEG) as those with a nominal $p < 0.05$. We further termed a DEG as up-regulated if its $\log_2\text{FoldChange} > 0$ in the comparison or down-regulated if its $\log_2\text{FoldChange} < 0$.

Supplementary results and discussion

DUSP4- and 5xFAD-associated PTMs in the tau protein

Another hallmark in AD neuropathology are the neurofibrillary tangles, which are caused by the abnormally phosphorylated tau protein^{5,6}. Remarkably, we detected 26 PTM sites in the tau protein (Matp gene) across the samples (Supplementary Figure S12). Importantly, the majority of these PTMs are present in the database (UniProtKB at <https://www.uniprot.org/>). In addition, as shown in Supplementary Figure S12, some of the PTMs are significantly associated with DUSP4 or 5xFAD. Strikingly, again, most of the PTMs displayed an opposite directionality in their association with DUSP4 vs. 5xFAD in each sex (Supplementary Figure S12). For example, in male mice, the PTM (Mapt;S554) is up-regulated by DUSP OE, whereas it is down-regulated by 5xFAD (Supplementary Figure S12). Once again, these results suggested that DUSP4 OE might reverse the effects of the 5xFAD transgene on the phosphorylation of tau protein in mouse brain.

DEG and DEP signatures are often overlapped

In our previous work, we reported DUSP4- or 5xFAD-associated genes (mRNAs)². To gain insight into the consistency between the DEGs and DEPs, we inspected the overlap between the DEG and DEP signatures over each comparison in each sex. For 5xFADvsWT in female mice, DEGs and DEPs are overlapped significantly and in the same directionality (Supplementary Figure S13). For example, the up-regulated DEG (mDEG(+)) is highly significantly overlapped with the up-regulated DEP (mDEP(+)) signature (FE = 3.0, p.adj = 9.0e-47, Supplementary Figure S13), highlighting the concordance in change in expression between the mRNAs and proteins caused by 5xFAD.

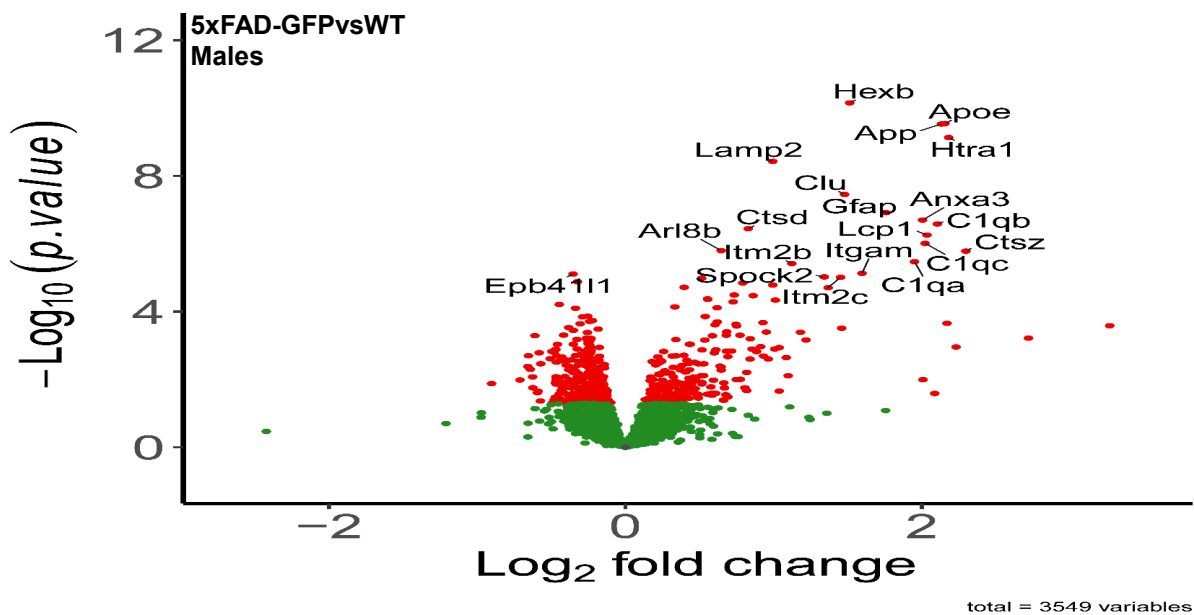
In 5xFAD-DUSP4vs5xFAD, down-regulated DEG and DEP signatures were significantly overlapped in female (Supplementary Figure S14A) and male mice (Supplementary Figure S14B). However, an insignificant overlap was found for the up-regulated DEG and DEP signatures albeit

we observed > 10 hits in overlap for each sex (p.adj is close to 0.2, Supplementary Figure S14).

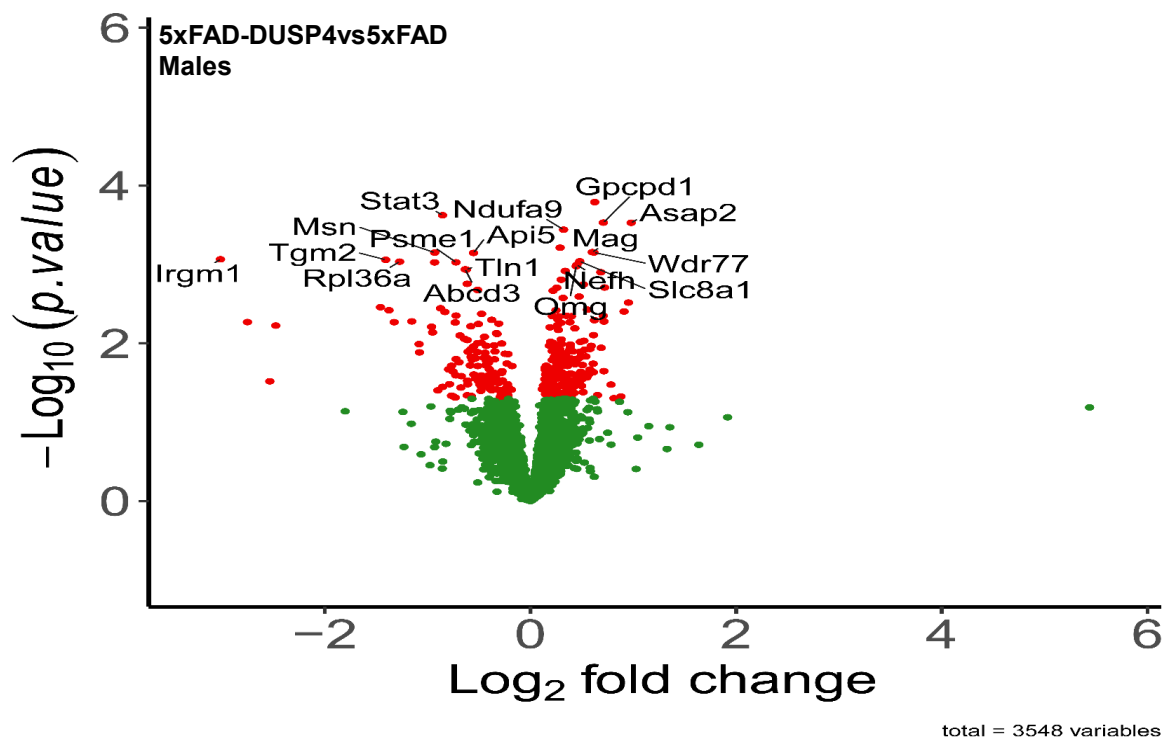
In contrast, for 5xFADvsWT in male mice, we did not observe significant overlaps between DEG and DEP signatures (data not shown). This might be due to that the RNA-seq assay is not sensitive enough to detect DEGs for this comparison in male at the time when the sampling took place or else any biological mechanism(s) underlying this discrepancy. Clearly, more future research is needed to clarify such inconsistency.

Supplementary Figures legends

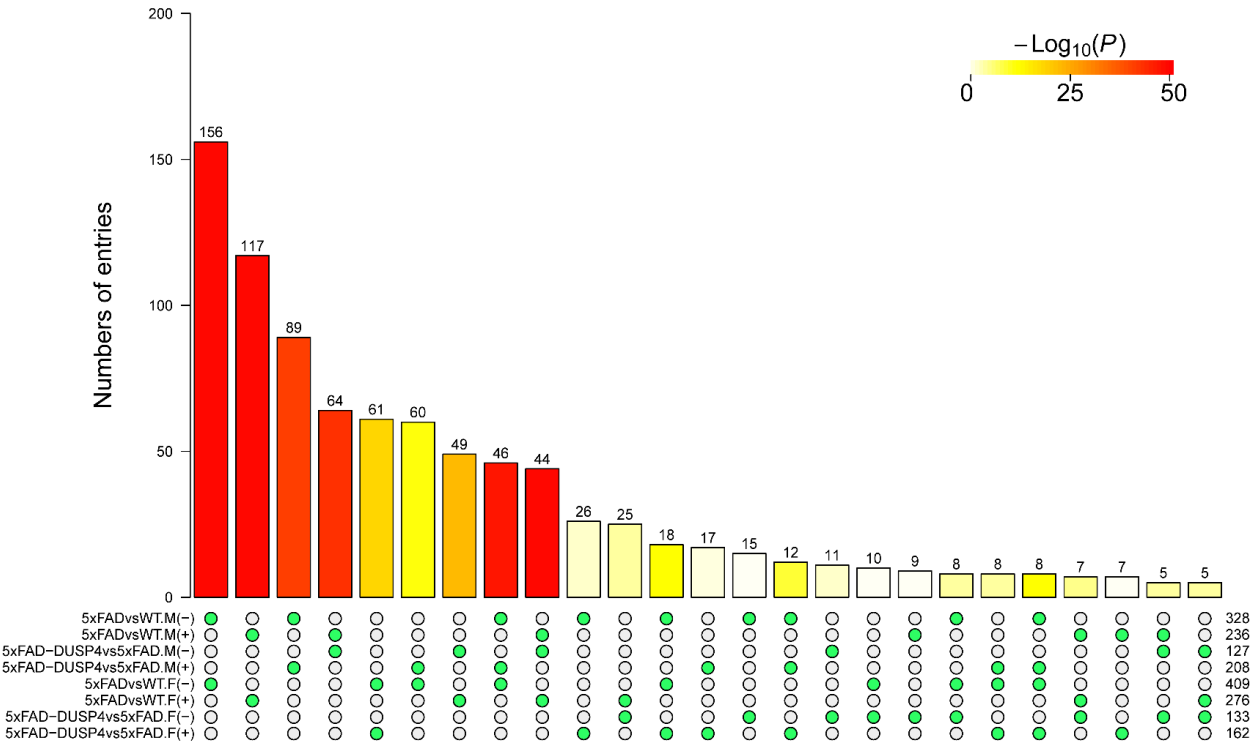
A



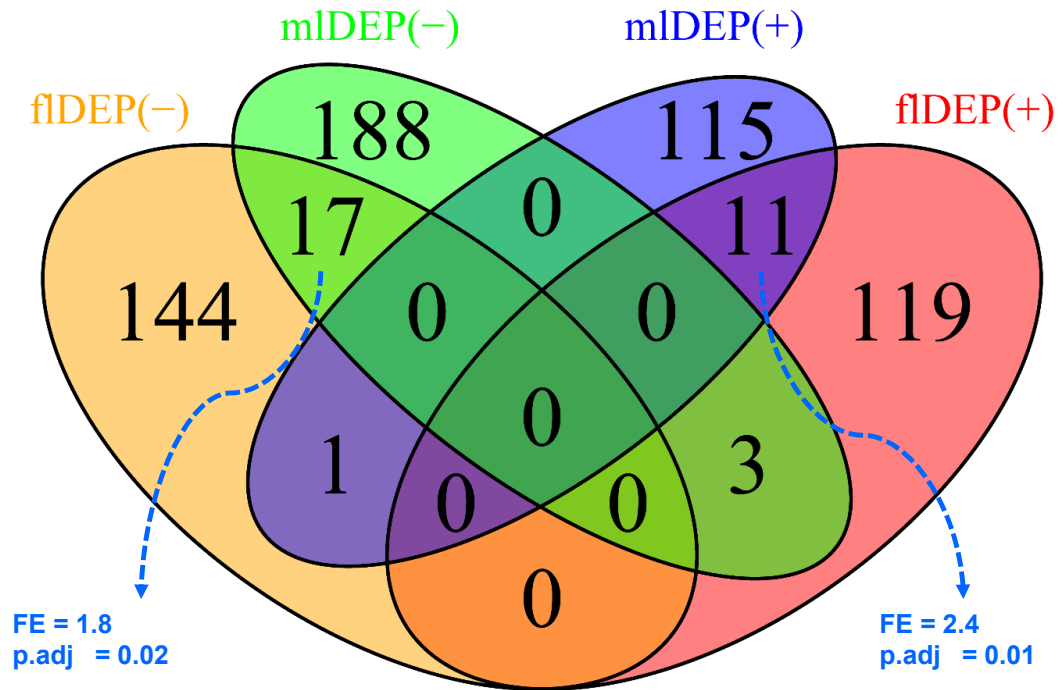
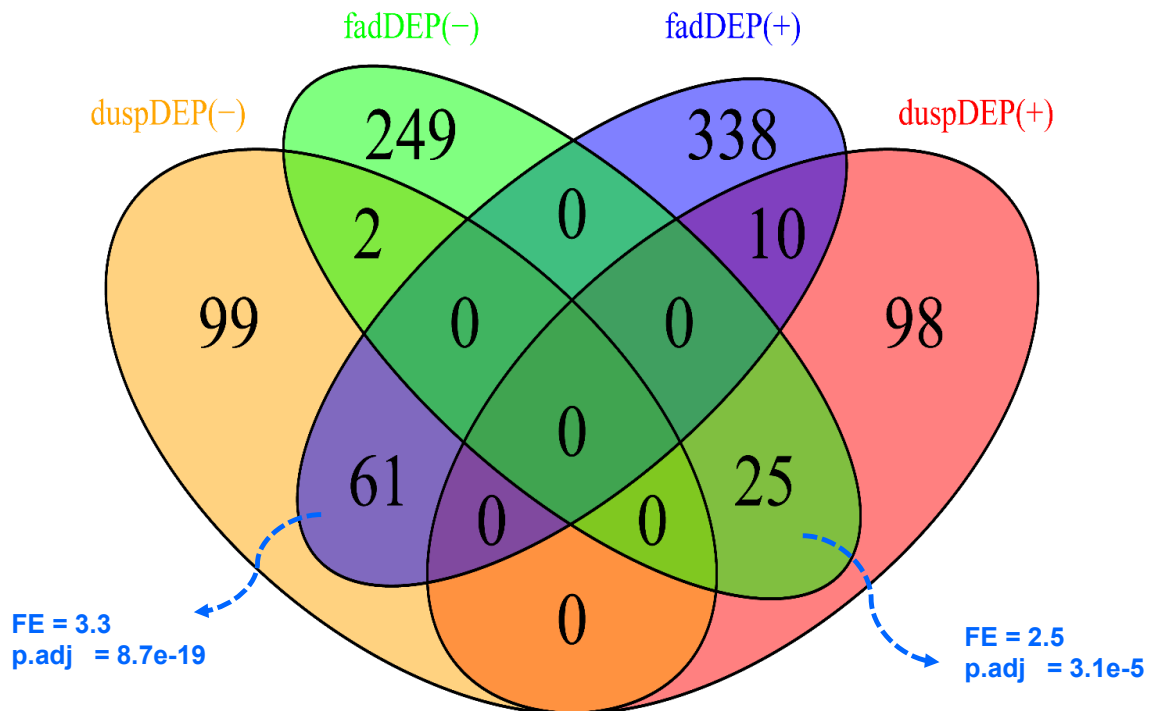
B



Supplementary Figure S1. Volcano plots for DEP analysis. (A) The DEPs in 5xFADvsWT in the male mice. (B) The DEPs in 5xFAD-DUSP4vs5xFAD in the male mice. Each dot represents a protein. Highlighted are top-ranked DEPs. Dots in red are DEPs, whereas dots in green are not differentially expressed proteins.



Supplementary Figure S2. Summary of the overlap and significance of the DEP signatures via the superExactTest. On the bottom of the bar graph, each row represents a DEP signature split by directionality in change in expression: - and +, down- and up-regulated, respectively. F and M, female and male, respectively. For example, 5xFADvsWT.M(-) stands for the down-regulated DEP signature in 5xFADvsWT in male mice. On the right are the numbers of the DEPs in each signature. Only shown here are the overlaps up to 3 groups. The number at the top of each bar is the number of DEPs overlapped among the groups (filled green circles) across rows under each bar. The color in each bar is proportional to the significance of the overlap ($-\log_{10}(P)$).

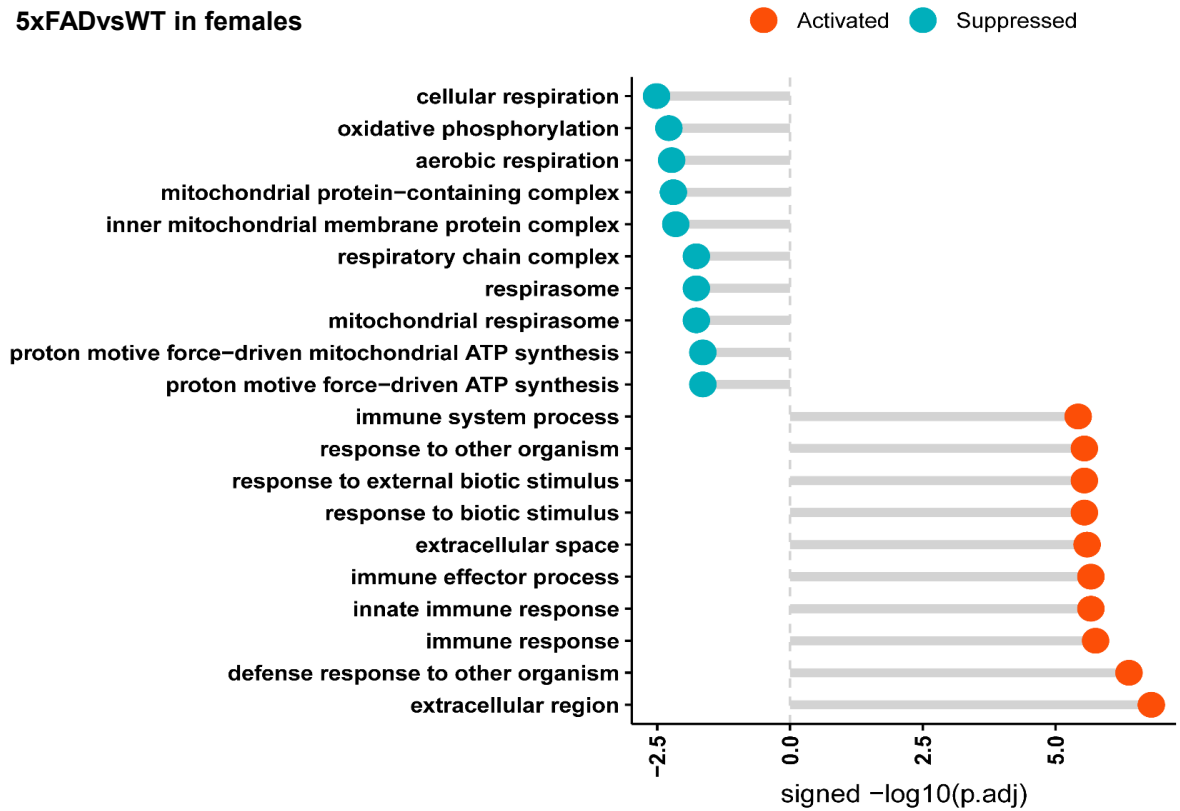
A**Male vs female in 5xFAD-DUSP4vs5xFAD****B****5xFAD-DUSP4vs5xFAD vs. 5xFAD-GFPvsWT in females**

Supplementary Figure S3. Venn diagrams highlighting the overlap of the DEP signatures.

(A) 5xFAD-DUSP4vs5xFAD in the male vs female mice. mlDEP(-) and mlDEP(+), are down- and up-regulated DEPs in males. flDEP(-) and flDEP(+), are down- and up-regulated DEPs in females. (B) Between 5xFAD-DUSP4vs5xFAD and 5xFADvsWT in the female mice. fadDEP(-) and fadDEP(+) are down- and up-regulated DEPs in 5XFAD. duspDEP(-) and duspDEP(+) are down- and up-regulated DEPs in DUSP4 OE. FE, fold enrichment. p.adj, BH-adjusted p value.

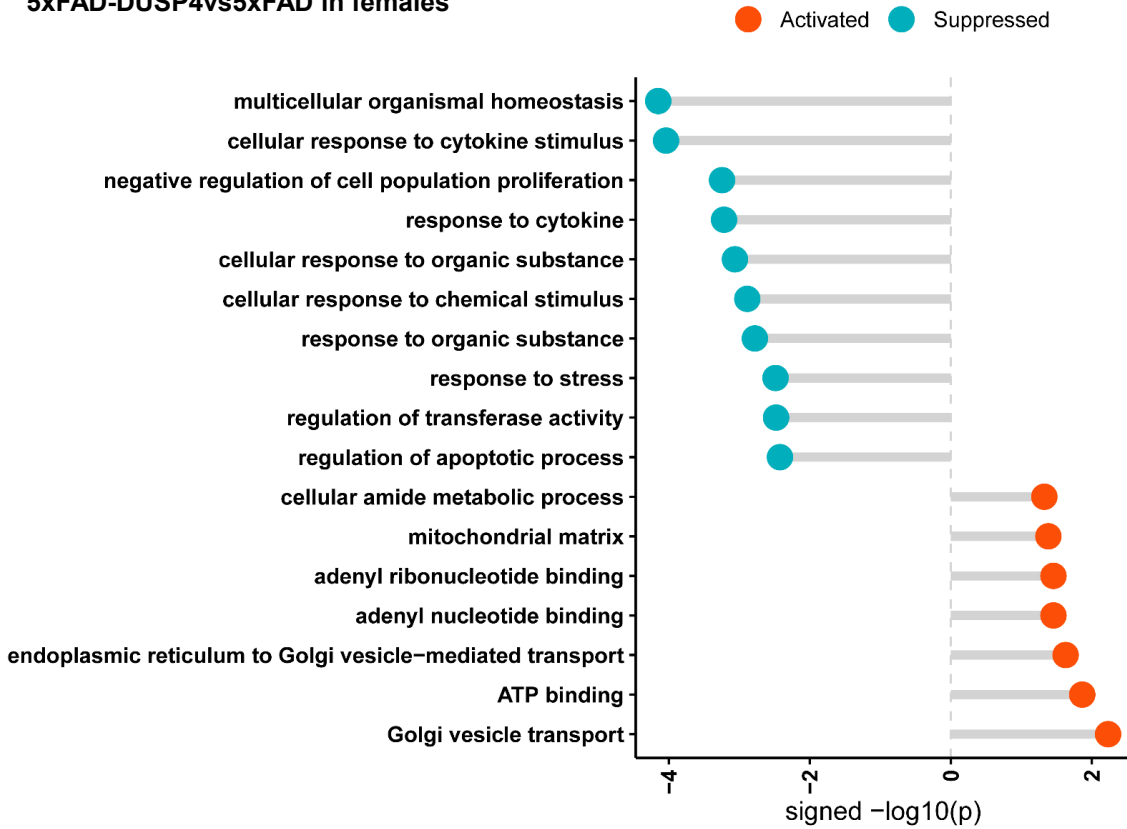
A

5xFADvsWT in females

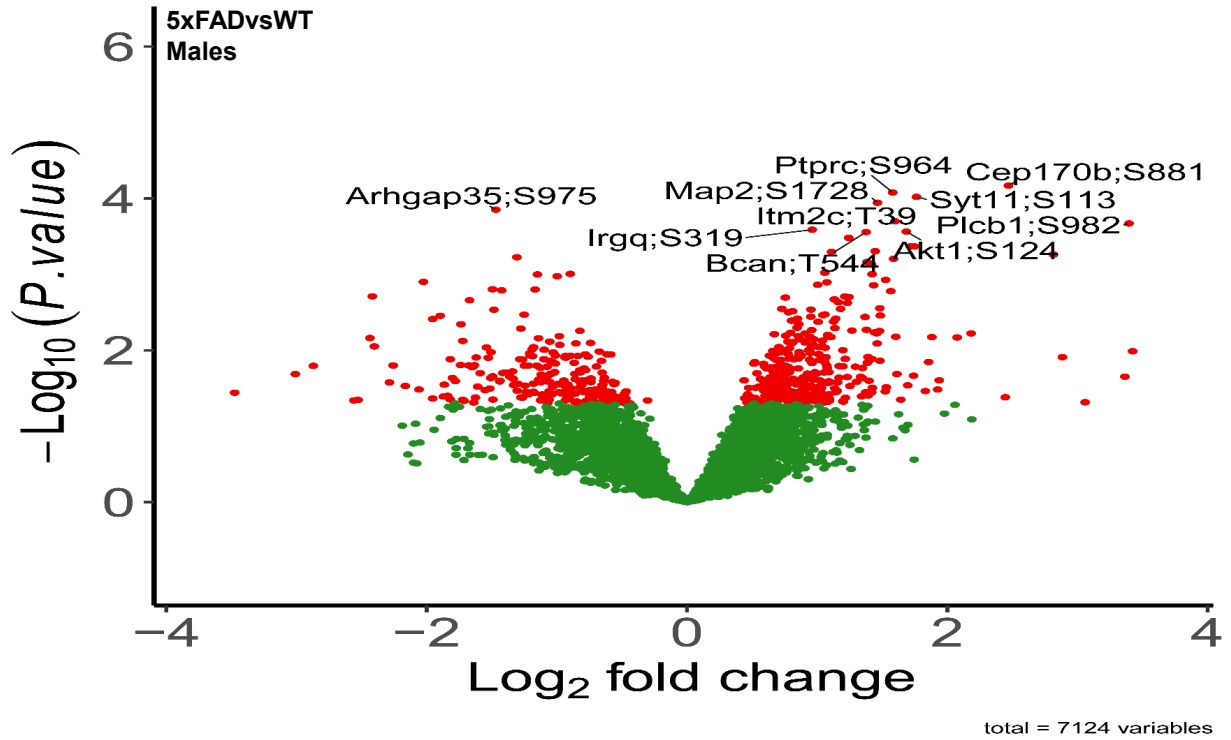


B

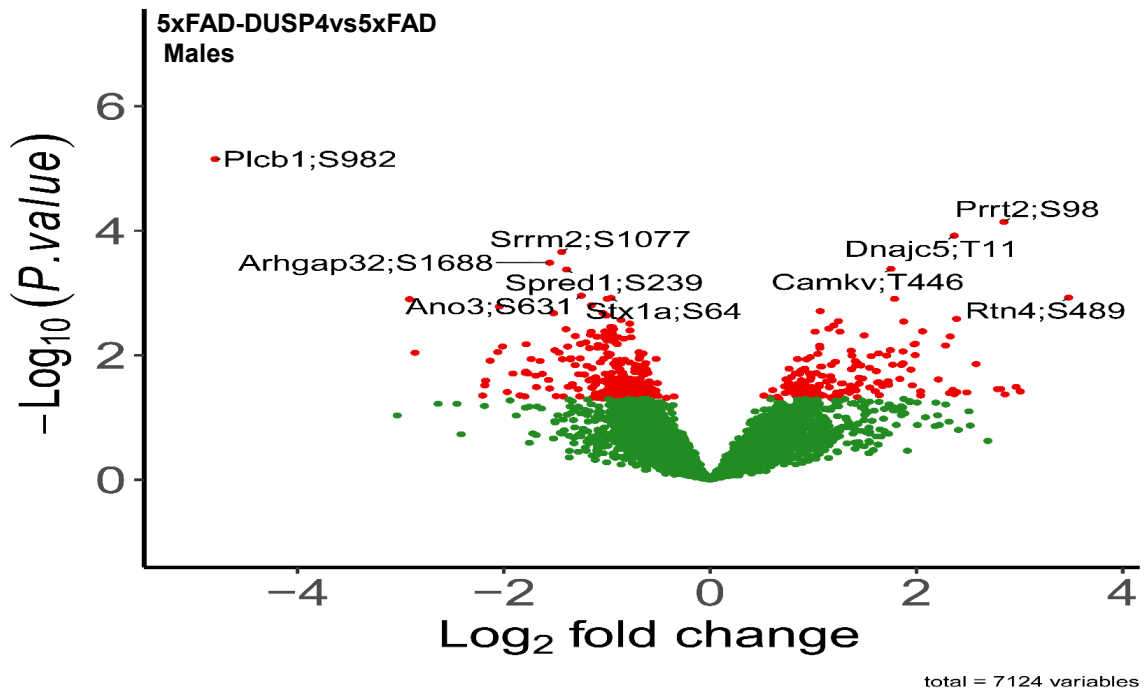
5xFAD-DUSP4vs5xFAD in females



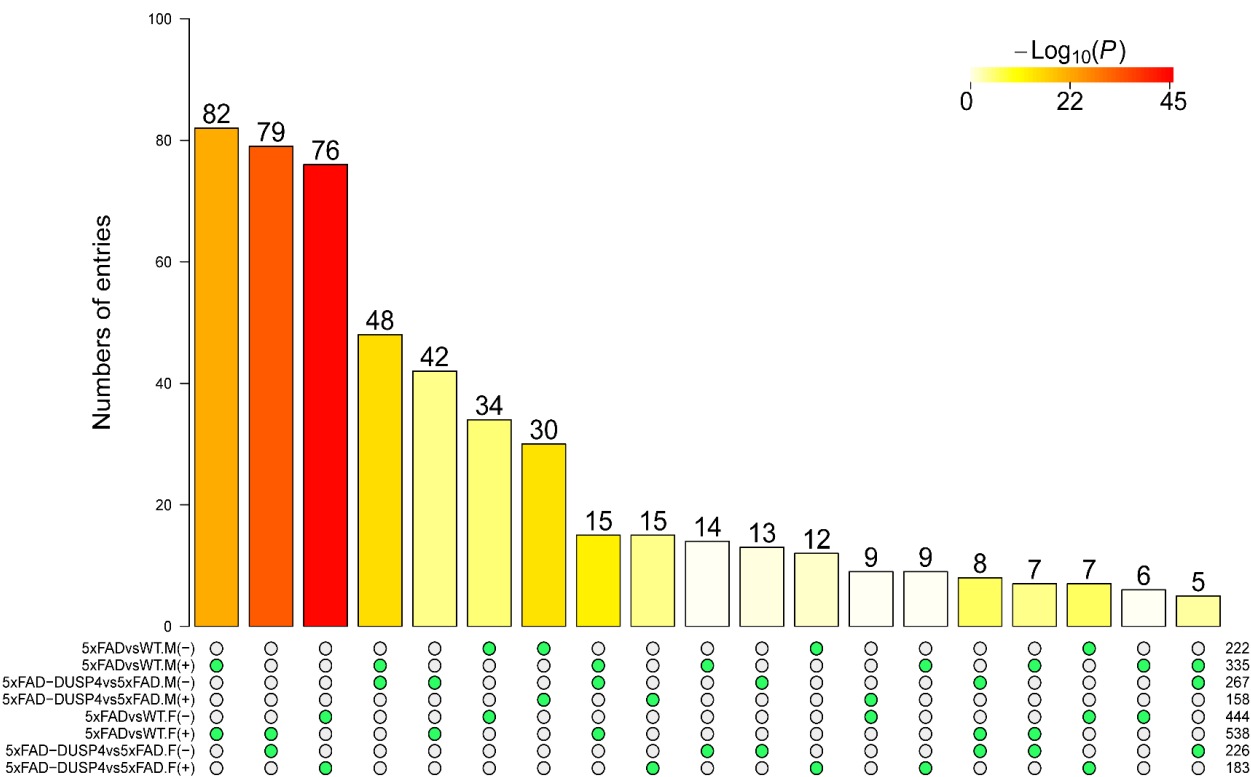
Supplementary Figure S4. GO enrichment analysis on the DEP signatures. (A) 5xFADvsWT in female mice. **(B)** 5xFAD-DUSP4vs5xFAD in female mice. GO terms are grouped by activated (in red) or suppressed (in turquoise). x-axis, $-\log_{10}(p.adj)$ **(A)** or $-\log_{10}(p)$ **(B)** split by enrichment groups, activated (positive) vs. suppressed (negative). y-axis, GO terms.



B



Supplementary Figure S5. Volcano plots for DEPTM analysis. (A) The DEPTMs in 5xFADvsWT in the male mice. (B) The DEPTMs in 5xFAD-DUSP4GFPvs5xFAD in the male mice. Each dot represents a PTM (phosphorylation) site. Highlighted are top-ranked PTMs (protein name and PTM site are connected by “;”). Dots in red are DEPTMs, whereas dots in green are not differentially expressed PTMs.

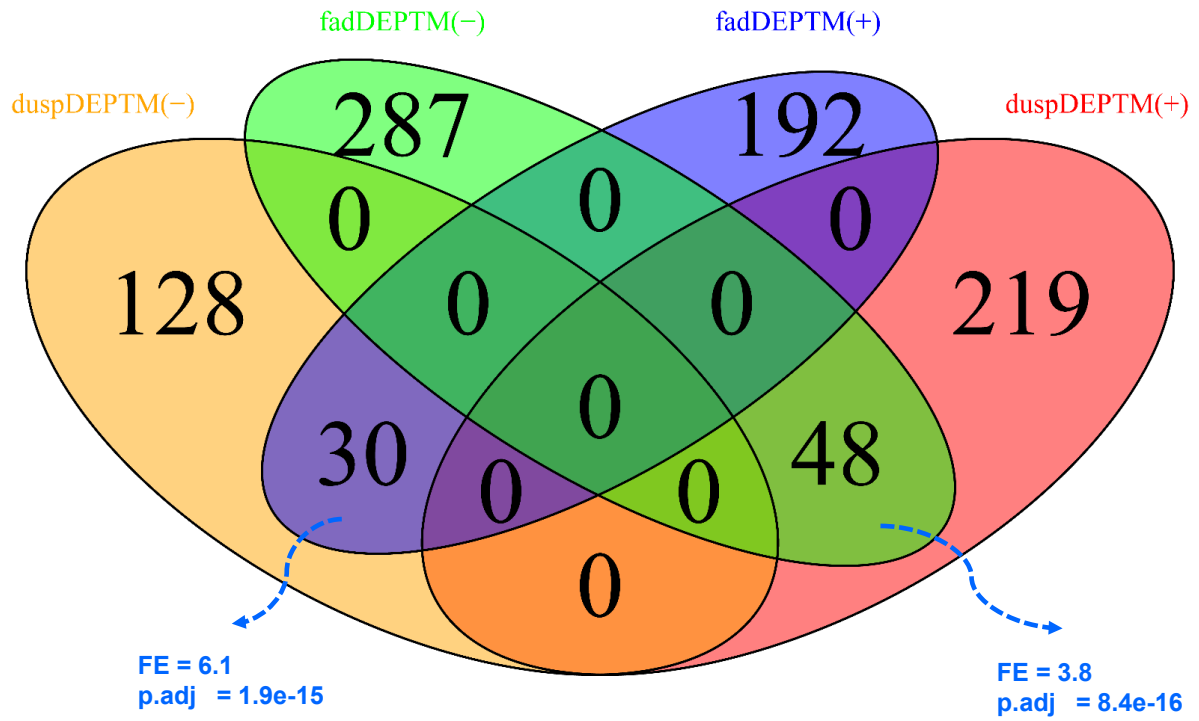


Supplementary Figure S6. Summary of the overlap and significance of the DEPTM signatures via the superExactTest. On the bottom of the bar graph, each row represents a DEPTM signature split by directionality in change in expression: - and +, down- and up-regulated, respectively. F and M, female and male, respectively. For example, 5xFADvsWT.M(-) stands for the down-regulated DEPTM signature in 5xFADvsWT in male mice. On the right are the numbers of the DEPTMs in each signature. Only shown here are the overlaps up to 3 groups. The number at the top of each bar is the number of DEPTMs overlapped among the groups (filled green circles)

across rows under each bar. The color in each bar is proportional to the significance of the overlap ($-\log_{10}(P)$).

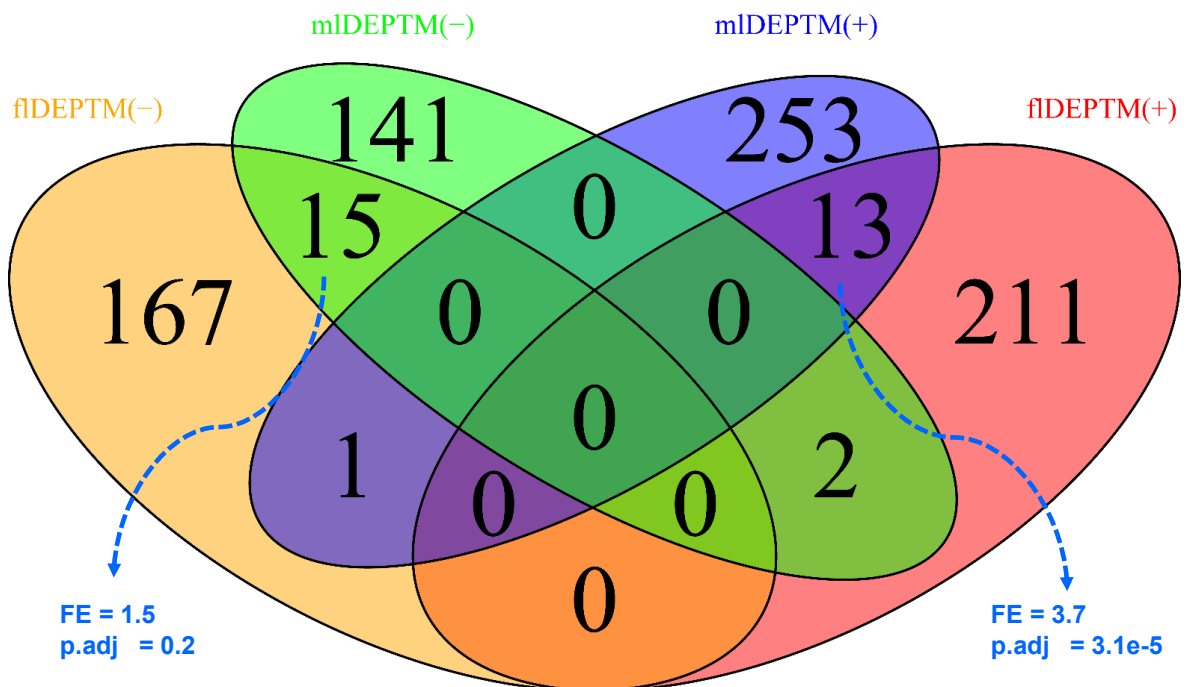
A

5xFAD-DUSP4vs5xFAD vs. 5xFAD-GFPvsWT in males



B

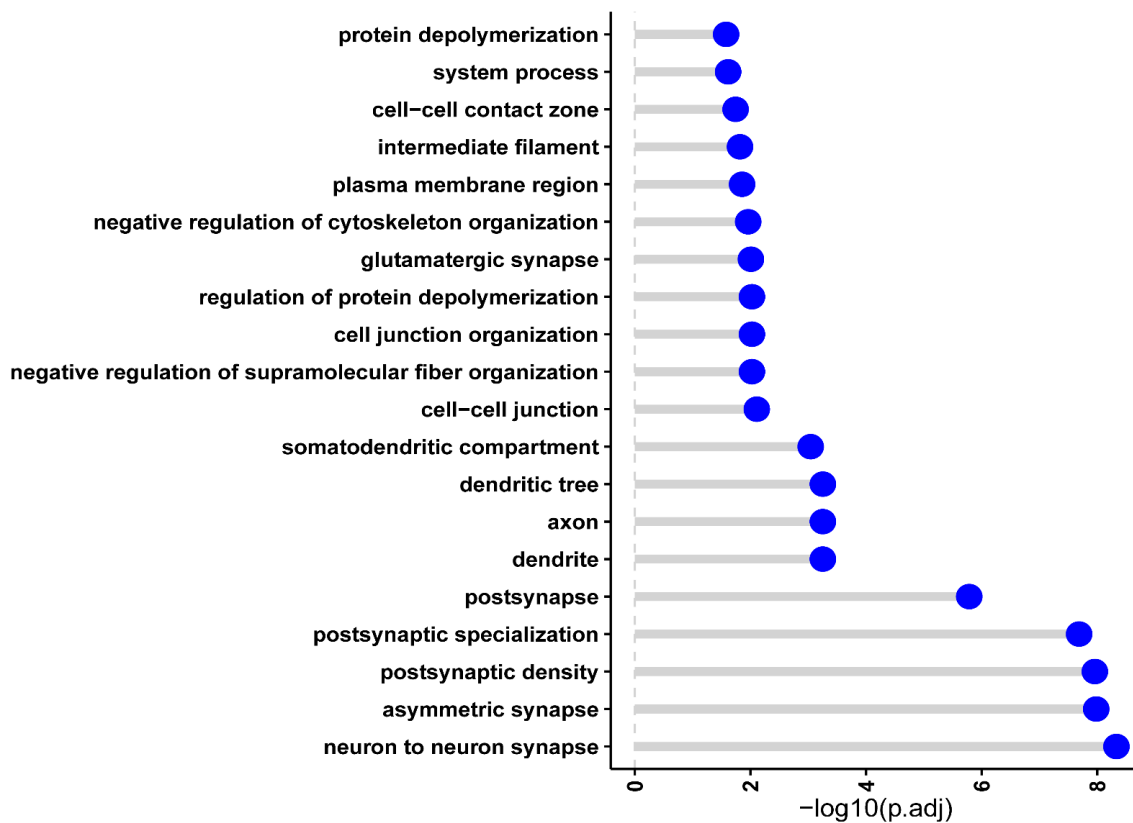
5xFAD-DUSP4vs5xFAD in male vs female



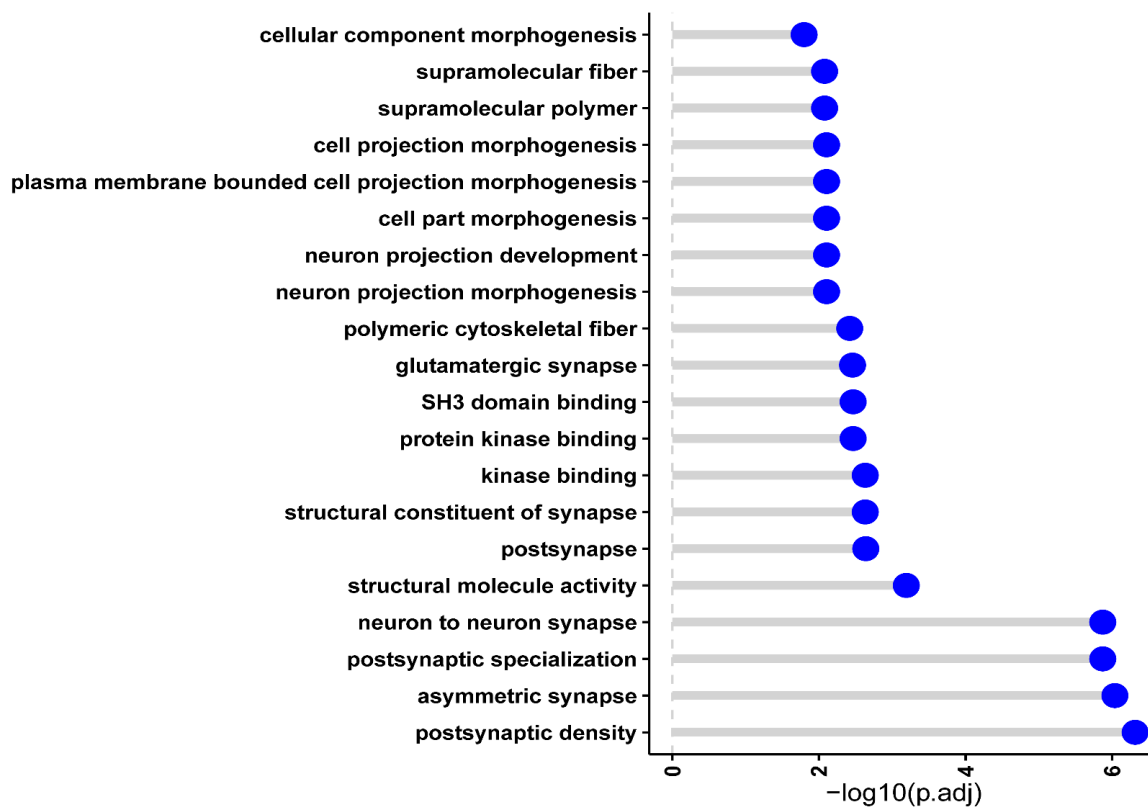
Supplementary Figure S7. Venn diagrams highlighting for the overlap of DEPTM signatures.

(A) Between 5xFAD-DUSP4vs5xFAD and 5xFADvsWT in the male mice. fadDEPTM(-) and fadDEPTM(+) are down- and up-regulated DEPTMs in 5XFAD. duspDEPTM(-) and duspDEPTM(+) are down- and up-regulated DEPTMs in DUSP4 OE. (B) 5xFAD-DUSP4vs5xFAD in the male vs female mice. mlDEPTM(-) and mlDEPTM(+), are down- and up-regulated DEPTMs in male. flDEPTM(-) and flDEPTM(+), are down- and up-regulated DEPTMs in female. FE, fold enrichment. p.adj, BH-adjusted p value.

A 5xFAD-GFPvsWT in males



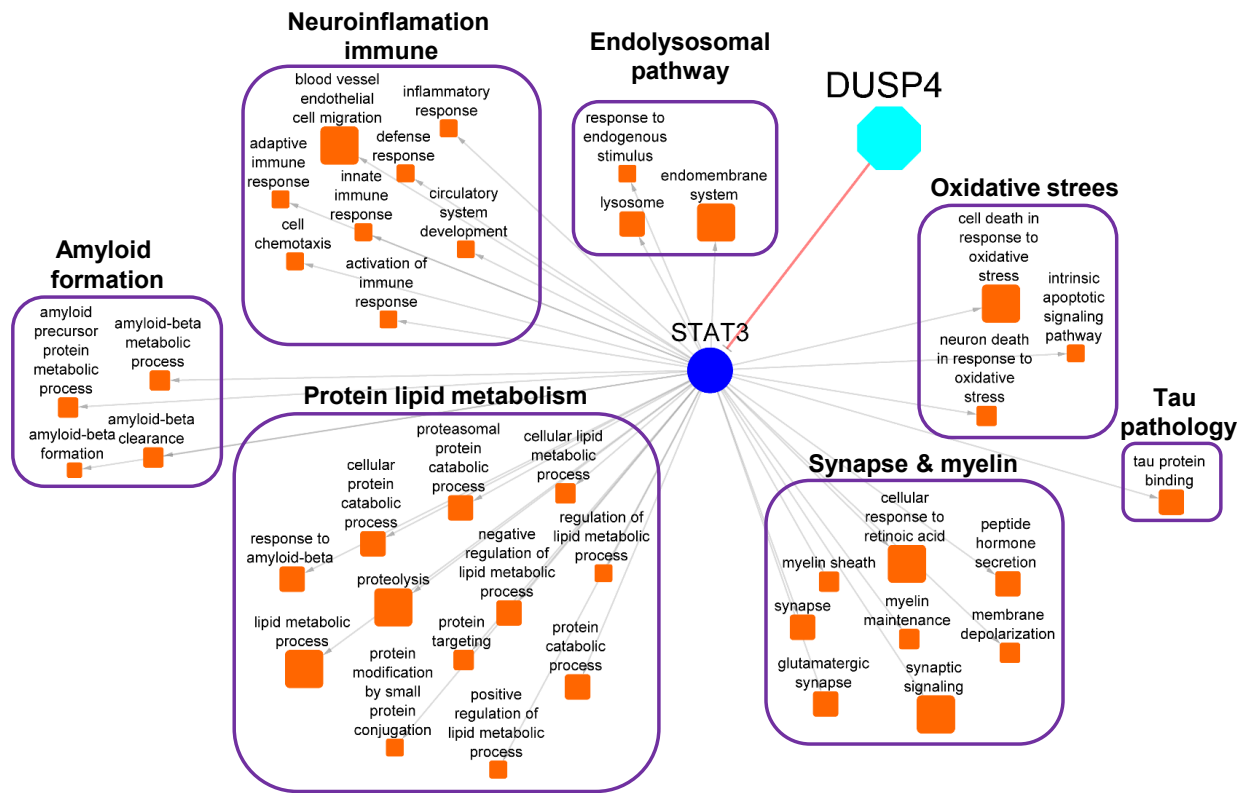
B 5xFAD-DUSP4vs5xFAD in males



Supplementary Figure S8. GO enrichment analysis on the DEPTM signatures. (A)

5xFADvsWT in male mice. (B) 5xFAD-DUSP4vs5xFAD in male mice. DEPTMs were collapsed across each protein. y-axis, GO terms. x-axis, $-\log_{10}(p.\text{adj})$.

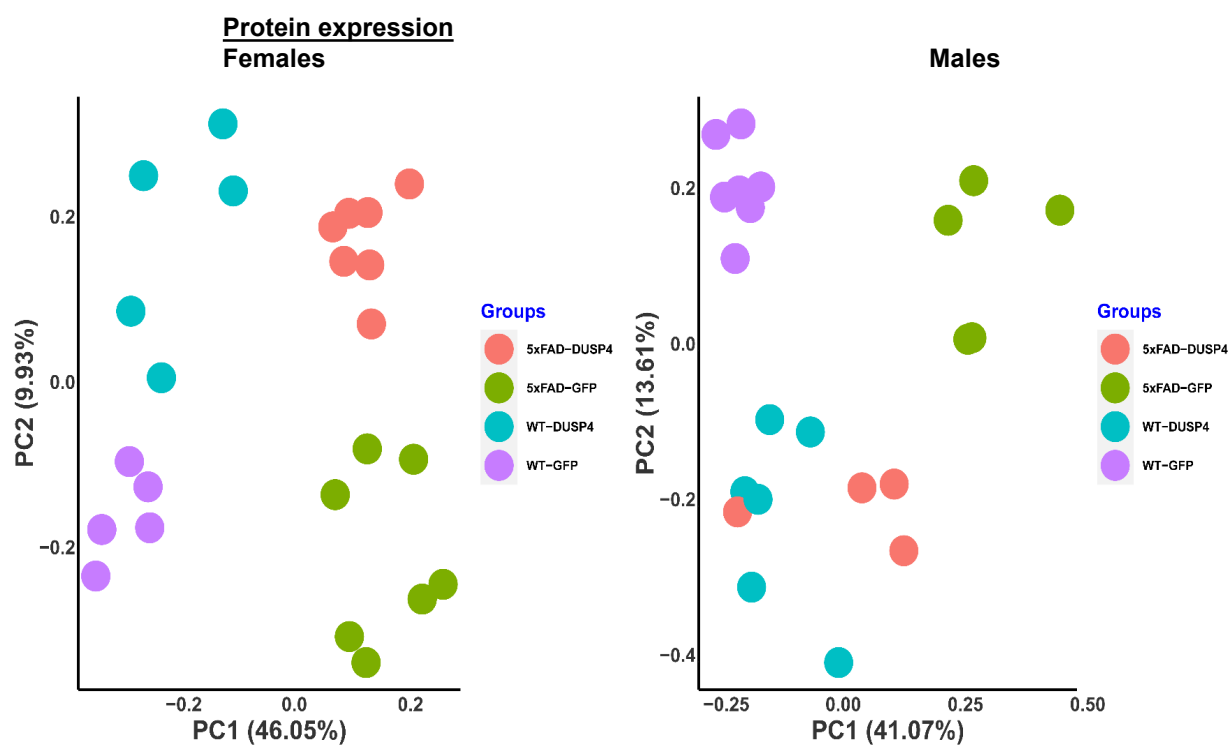
Supplementary Figure S9. Venn diagrams highlighting for the overlap of the DEP signatures between human and mouse. (A) Venn diagram revealing the overlap between the male mouse DEPs in 5xFAD-DUSP4vs5xFAD and the human male-specific DEPs in AD vs NL. (B) Venn diagram showing the overlap between the female mouse DEPs in 5xFAD-DUSP4vs5xFAD and the human female-specific DEPs in AD vs NL. In (A) and (B), mDEP(+) and mDEP(-), stand for up- and down-regulated DEPs in mice, respectively, whereas hDEP(+) and hDEP(-), stand for up- and down-regulated DEPs in human, respectively.



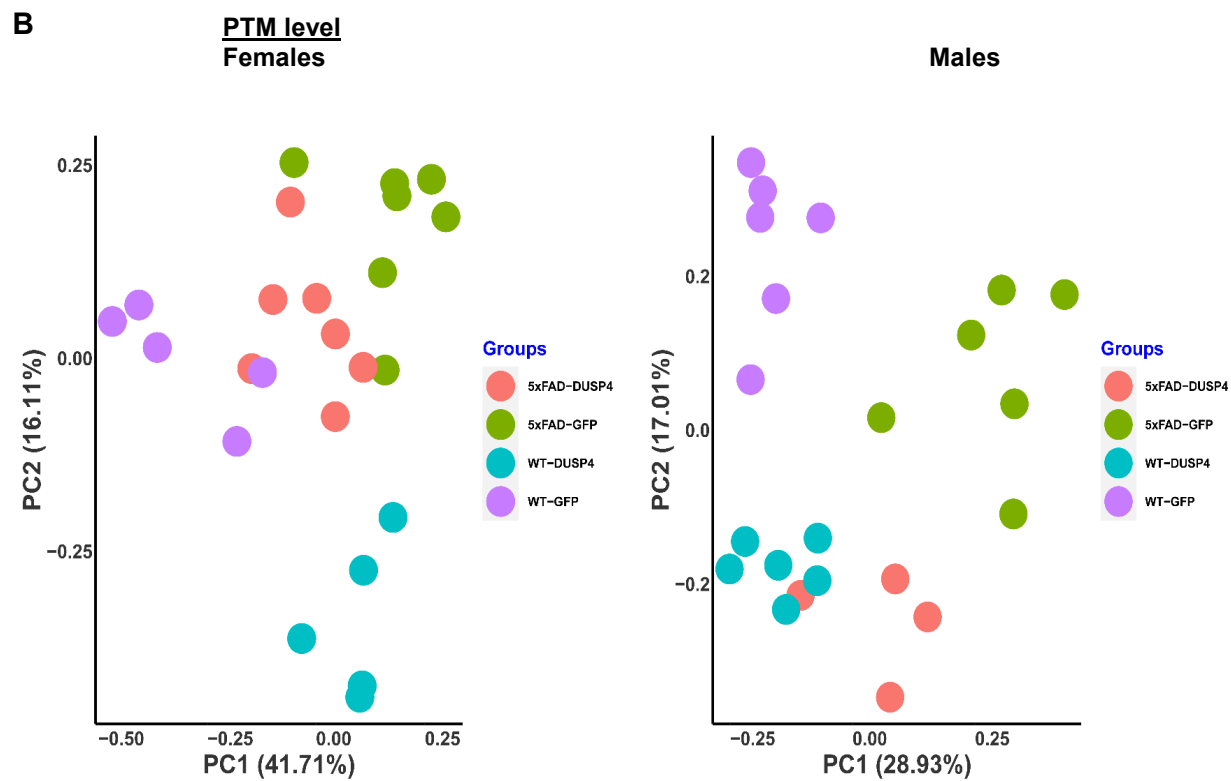
Supplementary Figure S10. The DUSP4-STAT3 protein signal map. The protein and protein interaction (PPI) subnetwork of STAT3 was obtained by querying the global PPI network⁷ (kindly gift from Dr. Feixiong Cheng) up to 1 undirected walk. The STAT3 protein subnetwork was overlapped with the AD-related GO pathways^{8,9} for enrichment, and thereby the DUSP4-STAT3 signal map was constructed (see Methods). Each filled box stands for a GO term, whose size is

proportional to its enrichment for the STAT3 subnetwork with a GO term. Large unfilled box are for the parent categories of GO terms in AD.

A



B

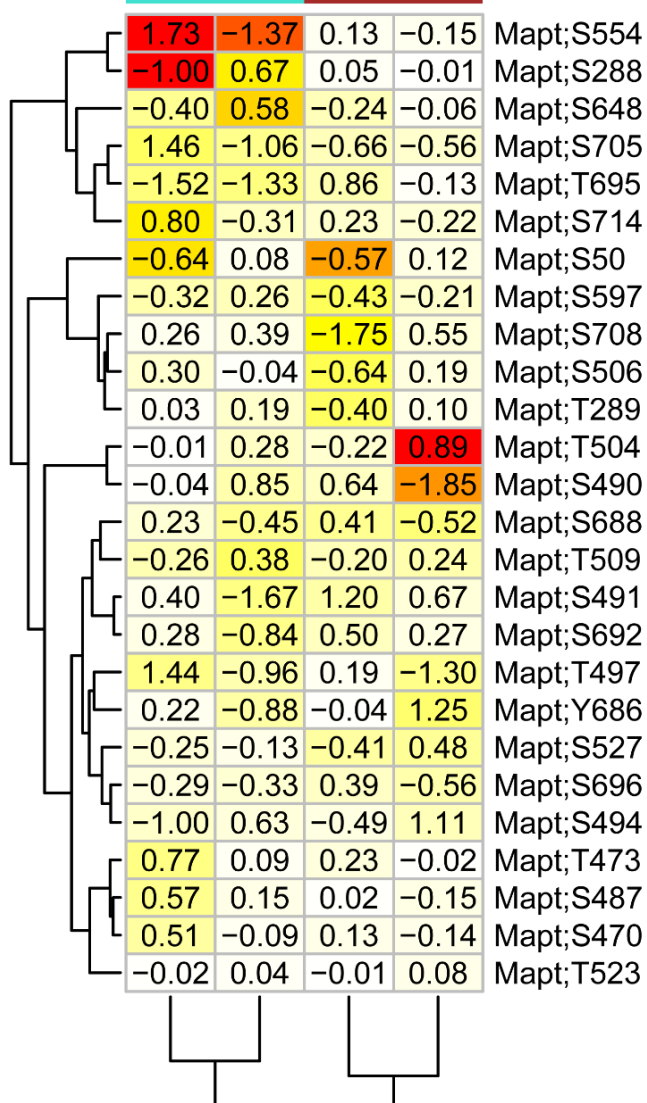


Supplementary Figure S11. PCA analysis of the protein and phosphoprotein expression.

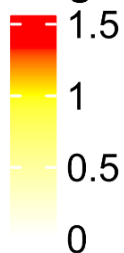
(A) The protein expression in the male (right panel) and female mice (left panel). (B) The phosphoprotein expression in the male (right panel) and female mice (left panel). Overall, the 4 experimental groups of mice can be classified by their genotype groups via PCA.

5xFAD-DUSP4vs5xFAD
5xFADvsWT
5xFAD-DUSP4vs5xFAD
5xFADvsWT

gender



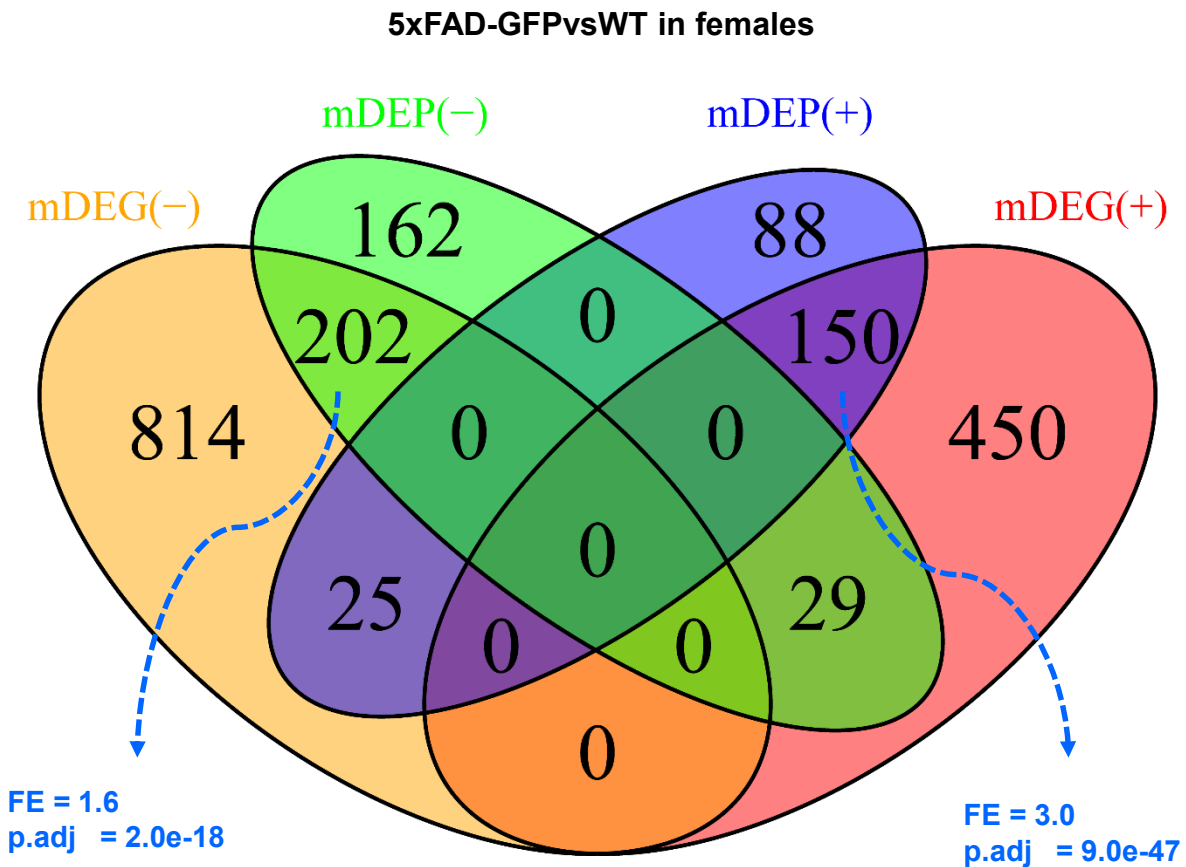
$-\log_{10}(p)$



gender

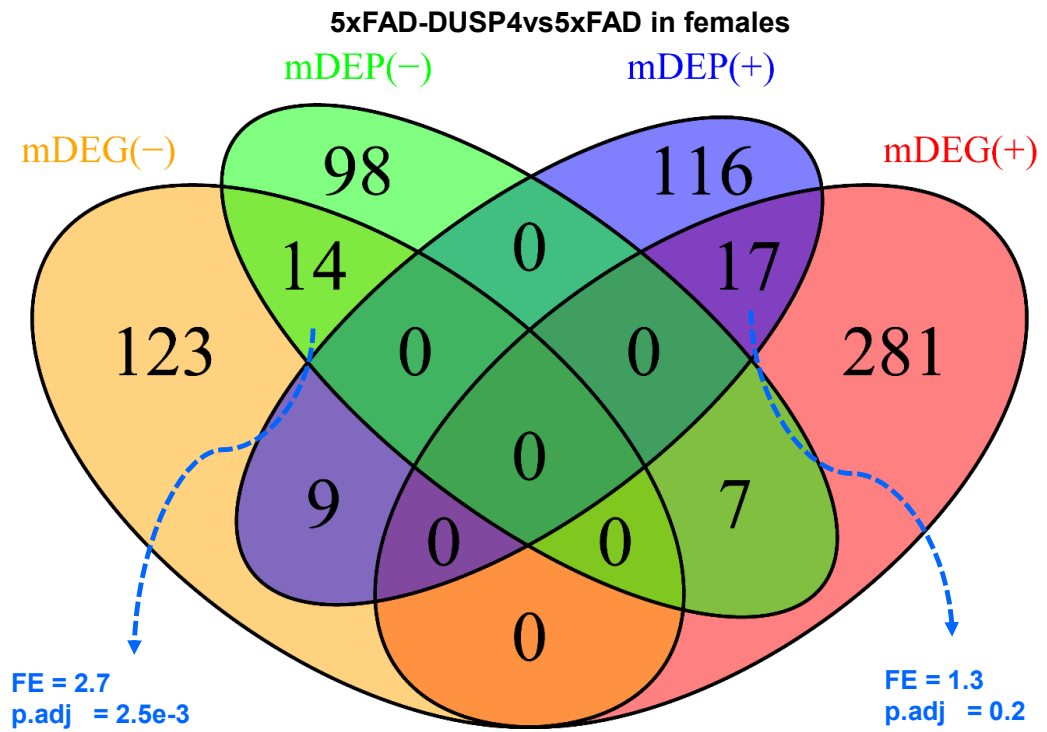


Supplementary Figure S12. Heatmap showing the significance and change in expression of PTMs in the tau protein (Mapt gene). The color intensity denotes and is proportional to the $-\log_{10}(p)$, where p is the statistic p value in each comparison. Highlighted numbers are the fold change in expression in each comparison.

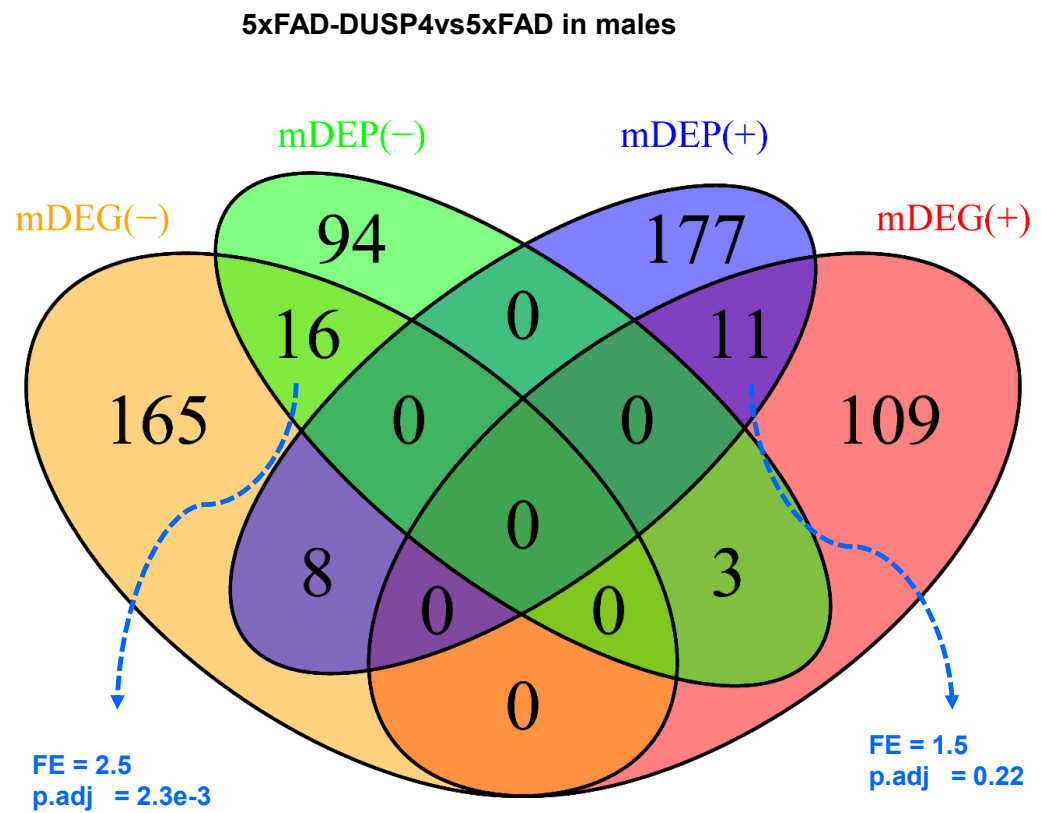


Supplementary Figure S13. Venn diagram highlighting for the overlap between DEP and DEG signatures for 5xFADvsWT. mDEP(-) and mDEP(+), are down- and up-regulated DEPs in females, respectively. mDEG(-) and mDEG(+), are down- and up-regulated DEGs in females, respectively. FE, fold enrichment. p.adj, BH-adjusted p value.

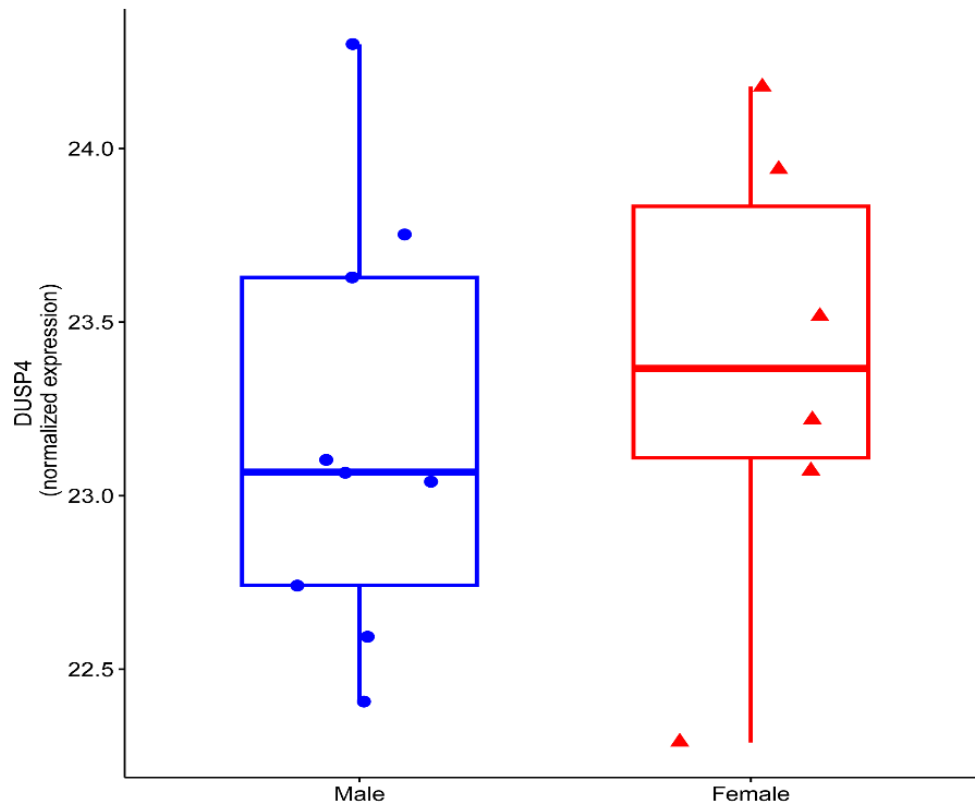
A



B



Supplementary Figure S14. Venn diagrams highlighting for the overlap between DEP and DEG signatures for 5xFAD-DUSP4vs5xFAD. (A) female mice; (B) male mice. mDEP(-) and mDEP(+), are down- and up-regulated DEPs, respectively. mDEG(-) and mDEG(+), are down- and up-regulated DEGs, respectively. FE, fold enrichment. p.adj, BH-adjusted p value.



Supplementary Figure S15. Boxplots showing DUSP4 protein expression in male vs. female mice in the proteomic profiling. We pooled the mice of both sexes that are either WT-DUSP4 or 5xFAD-DUSP4, and then tested the difference of DUSP4 expression between male and female mice using student's t test. The difference in DUSP4 protein level is not statistically significant ($p = 0.59$). $n = 9$ and 6 for male and female mice, respectively.

Supplementary Data

Supplementary.data1.xlsx

Supplementary.data2.xlsx

Supplementary.data3.xlsx

Supplementary.data4.xlsx

References

- 1 Seyfried, N. T. *et al.* A Multi-network Approach Identifies Protein-Specific Co-expression in Asymptomatic and Symptomatic Alzheimer's Disease. *Cell Syst* **4**, 60-72 e64, doi:10.1016/j.cels.2016.11.006 (2017).
- 2 Pan, A. L. *et al.* Dual-Specificity Protein Phosphatase 4 (DUSP4) Overexpression Improves Learning Behavior Selectively in Female 5xFAD Mice, and Reduces beta-Amyloid Load in Males and Females. *Cells* **11**, doi:10.3390/cells11233880 (2022).
- 3 Love, M. I., Huber, W. & Anders, S. Moderated estimation of fold change and dispersion for RNA-seq data with DESeq2. *Genome Biol* **15**, 550, doi:10.1186/s13059-014-0550-8 (2014).
- 4 Zhu, A., Ibrahim, J. G. & Love, M. I. Heavy-tailed prior distributions for sequence count data: removing the noise and preserving large differences. *Bioinformatics* **35**, 2084-2092, doi:10.1093/bioinformatics/bty895 (2019).
- 5 Hardy, J. The amyloid hypothesis for Alzheimer's disease: a critical reappraisal. *J Neurochem* **110**, 1129-1134, doi:10.1111/j.1471-4159.2009.06181.x (2009).
- 6 Huang, Y. & Mucke, L. Alzheimer mechanisms and therapeutic strategies. *Cell* **148**, 1204-1222, doi:10.1016/j.cell.2012.02.040 (2012).
- 7 Zhou, Y. *et al.* AlzGPS: a genome-wide positioning systems platform to catalyze multi-omics for Alzheimer's drug discovery. *Alzheimers Res Ther* **13**, 24, doi:10.1186/s13195-020-00760-w (2021).
- 8 Wang, E., Lemos Duarte, M., Rothman, L. E., Cai, D. & Zhang, B. Non-coding RNAs in Alzheimer's disease: perspectives from omics studies. *Hum Mol Genet* **31**, R54-R61, doi:10.1093/hmg/ddac202 (2022).
- 9 Neff, R. A. *et al.* Molecular subtyping of Alzheimer's disease using RNA sequencing data reveals novel mechanisms and targets. *Sci Adv* **7**, doi:10.1126/sciadv.abb5398 (2021).